An improvement of the too cold tongue in the tropical Pacific with the development of an ocean-wave-atmosphere coupled numerical model*

Song Zhenya, Qiao Fangli**, Yang Yongzeng and Yuan Yeli

(The First Institute of Oceanography, SOA, Qingdao 266061, China)

Accepted on October 23, 2006

Abstract A common problem in the application of the coupled ocean-atmosphere general circulation models (CGCMs) without flux correction is that the simulated equatorial cold tongue in general tends to be too strong, narrow, and extending too far west. The causes are not well understood yet. One possible reason may be the simulated mixed layer depth (MLD) is too shallow in the tropical Pacific due to insufficient vertical mixing in the OGCM. It is believed that the wave-induced vertical mixing can greatly improve the simulation of the MLD and thermocline structure. In this study, the coupled ocean-atmosphere general circulation model (FGCM-0) incorporated with wave-induced mixing has been employed to simulate the tropical Pacific sea surface temperature (SST). Generally, the wave-induced mixing lowers the SST in the OGCM because the strengthened vertical mixing can bring more cold water upward. However, in the coupled model, the non-uniformity of the space distribution in SST drop generates a horizontal gradient of the sea surface air pressure, and thus yields surface wind field anomaly. The wind anomaly leads to both ocean surface circulation anomaly and downwelling anomaly, which can restrain the overly-westward extension of the cold tongue in the tropical Pacific. Compared with the model results from the original model (FGCM-0), the modeled SST is higher by more than 0.8℃, with a maximum of 1.2℃ in the western Pacific (160—180°E, 0—3°N). The eastern boundary of the isotherm of 26.0℃ also moves from 165°E to 180°E. The overly westward extension of the simulated equatorial cold tongue is suppressed with the incorporation of the wave-induced mixing in the coupled model. The simulated SST shows in general improved results with a maximum improvement of more than 1.0℃. The simulated SST improvement in the north tropical Pacific is much better than that of the south tropical Pacific.

Keywords: cold tongue, wave-induced mixing, the coupled ocean-atmosphere general circulation models, the tropical Pacific

The tropical Pacific is a region with strong air-sea interactions, as evidenced by the occurrence of remarkable interannual signal such as ENSO event. The coupled ocean-atmosphere general circulation models (CGCMs) widely used in the global climate research can provide credible simulations of fundamental properties of the climate system such as the annual mean temperature and its seasonal cycles[1]. However, the simulation results of these coupled models are often unsatisfactory without the inclusion of appropriate flux corrections. One of the common problems is that the simulated sea surface temperature (SST) deviates noticeably from real observations in the tropical Pacific. Mechoso[2] compared the results of 11 CGCMs with real measurements and concluded that the simulated equatorial cold tongue in general tends to be too strong, too narrow, and extending too far west. By analyzing the results of 23 CGCMs, Davey[3] reported that the annual mean SST simulated by all CGCMs without flux correction is too cold in an equatorial 2°N—2°S strip at the western and central Pacific. In essence, without flux correction, the simulated cold tongue over the equator from most CGCMs is too cold, while that of the simulated SST in the southeast (SE) Pacific, northeast (NE) Pacific and southeast (SE) Atlantic[4—8] is too warm compared with real observations.

In order to reduce the systematic bias, flux adjustment technique has been developed[9—11]. This method takes into account the effects of the climatological observations including heat flux, SST and fresh water flux. Data assimilation is able to reduce the bias and improve the simulation of climatology fields[2,3,9—11]. However, these flux adjustments are empirical in nature, and the parameters used are difficult to relate to the actual physical processes in real world climate systems. They quite often lead to problems of non-conservations in heat and fresh water fluxes across the air-sea interface, and also torture the atmosphere and ocean dynamical processes[1,12,13]. Improving the spatial resolution can reduce the system bias, but the effects are not obvious for the global

* Supported by National Natural Science Foundation of China (Grant No. 40476017) and the National Key Basic Research Projects (2006CB403605)

** To whom correspondence should be addressed. E-mail: qiaofl@fio.org.cn

simulation, and the problem of an overly cold and overly westward extended cold tongue still remains in the modeling results[4,8].

Covey et al.[1] attributed the bias of SST simulation to two problems, namely, the coupling flux error, and inaccurate parameterizations or accumulation of numeric errors. Philander[14] proposed that the cause of the systematic errors may be caused by the omission of some crucial air-sea feedback mechanisms in the model. However, the exact processes which are involved in these feedback mechanisms are by no means clear. Zhang et al.[17] suggested that the cause of the biases found in the result of the flexible coupled ocean-atmosphere general circulation model (FGCM-0) is probably related to a combination of two factors. The first is the excessive shallowness of the thermocline and MLD at the equator and the south Pacific, and the second is the non-ideal vertical mixing scheme owing to the sharp and abrupt dropping of the vertical mixing rate with depth.[2,4]

The estimated energy input through Ekman layer contains two parts, i.e., 0.5—0.7 TW in near-inertial frequency[18] and 2.4 TW in the sub-inertial frequency range[19]. The energy input through geostrophic current is 1.3 TW[20], while the input through surface wave is 60 TW[19]. In other words, the surface wave contains much more energy than that of ocean circulation. The wave-induced vertical viscosity/diffusivity Bv has been analytically expressed as a function of wave number spectrum[21], and Bv can be rewritten to be the function of Stocks drift if regarding the surface wave as a monochromic wave[1)]. The energy input from the surface wave to the general circulation can improve dramatically the simulation of the global upper mixed layer in an ocean general circulation model. For example, the section-mean correlation coefficient between the model results and the Levitus data, from surface to 100 m along the 35°N section of both the Pacific and Atlantic oceans, is improved from 0.68 without wave effect to 0.93 with wave effect. In this study, we have added Bv, wave-induced vertical mixing, into the coupled ocean-atmosphere general circulation model (CGCM), FGCM-0. Our focus has been placed on the simulation of SST in the tropical Pacific covering the area of 120°E—60°W and 25°S—25°N, with the primary aim to gain better understanding on how the surface wave affects the simulation of the cold tongue.

1 Model descriptions

The coupled ocean-atmosphere general circulation model used is the flexible coupled ocean-atmosphere general circulation model (referred to as FGCM-0), which was developed at the Institute of Atmospheric Physics (IAP), Chinese Academy of Sciences (CAS). FGCM-0 is based on the NCAR climate system model, version 1 (NCAR CSM-1)[7] with the replacement of the original ocean circulation model, NCOM, by the L30T63[23,24]. The other components are almost the same as those in the CSM-1. Different from the CSM-1, the coupling of fresh water exchange is replaced by the relaxation condition of salinity. The atmosphere component is the community climate model, version 3 (CCM3)[25], and the horizontal resolution is T42. The oceanic component is the global OGCM, L30T63 developed by Jin et al.[23]. Its horizontal grid is exactly the same as that of a T63 AGCM, about 1.875°× 1.875°. The "PP" scheme for the upper ocean vertical mixing and the isopycnal mixing scheme proposed by Gent and MacWilliams is adapted[26]. The atmospheric, land, and sea ice models communicate with the flux coupler at a rate of every model hour, and the oceanic model does this at a rate of every model day. As the CSM-1, the models in the FGCM-0 are directly coupled by exchanging the heat and momentum fluxes. Compared to the observed climatology, although the model simulates the double ITCZ and the "too cold" tongue, the model does not show obvious climate drift and could reproduce satisfactorily the basic features of the atmosphere and oceanic circulation. For further details of the FGCM-0, see Ref. [16].

Based on the MASNUM wave number spectral model, Qiao et al.[21] developed an expression of wave-induced mixing Bv as a function of wave number spectrum,

$$Bv = \alpha \iint_k E(\boldsymbol{k}) \exp\{2kz\} \mathrm{d}\boldsymbol{k} \frac{\partial}{\partial z} \cdot \left(\iint_k \omega^2 E(\boldsymbol{k}) \exp\{2kz\} \mathrm{d}\boldsymbol{k} \right)^{1/2}$$

where $E(\boldsymbol{k})$ represents the wave number spectrum, ω the wave angular frequency, k the wave number, z the vertical coordinate axis upward positive with $z=0$ at the surface, and α is a constant.

1) Qiao FL, Fang GH, Xia CS, et al. The role of surface waves in the ocean mixed layer. Science in China (submitted).

The MASNUM (once called LAGFD-WAM) wavenumber spectrum numerical model[28,29] was used to compute Bv with $\alpha = 1$. The numerical wave model has been calibrated and adopted many times in offshore engineering studies[21,30—32]. The computational domain is 75°S—65°N, 0—360°E with a horizontal resolution of 0.5°×0.5°. The National Center for Environmental Prediction (NCEP) reanalyzed wind fields of 2001 with the horizontal resolution of 1.25°×1.0° and a time interval of 6 hours. The wind field interpolated into the model grid was used to calculate the wave number spectrum, and the calculated Bv was then used in the CGCM annual circularly.

In the study area within 120° E—60° W and 25°S—25°N, the maximum of the annual-mean Bv at sea surface is 443 $cm^2 s^{-1}$ (Fig. 1(a)). The annual mean Bv of the top 20 m averaged is about 20 $cm^2 s^{-1}$ along the equator, and increases with distance from the equator towards higher latitudes. The maximum is about 100 $cm^2 s^{-1}$ at the south and north boundaries. Bv is a little weaker in the central Pacific than those of west and east Pacific. Fig1. (b), (c) and (d) show respectively the distributions of wave-induced mixing along the equator, the 10° S and the 10°N transects.

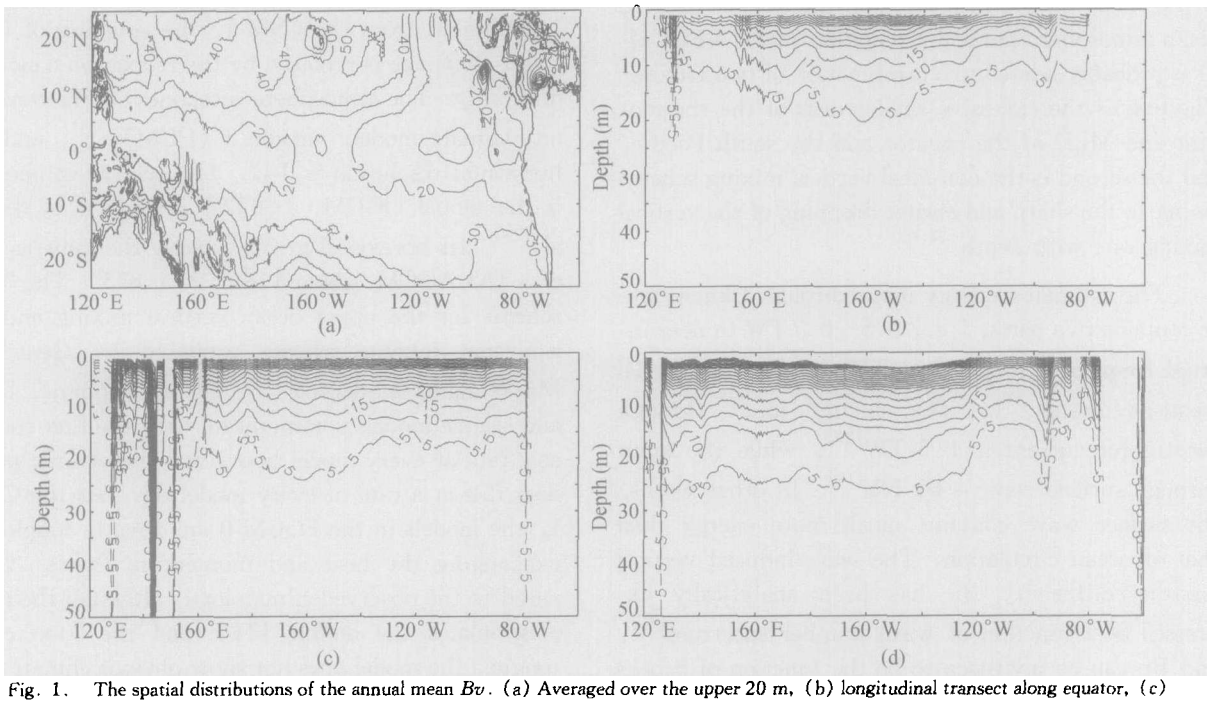

Fig. 1. The spatial distributions of the annual mean Bv. (a) Averaged over the upper 20 m, (b) longitudinal transect along equator, (c) longitudinal transect along 10°S, (d) longitudinal transect along 10°N.

The wave-induced vertical mixing could be added to ocean circulation model as a part of the vertical kinematic viscosity and vertical diffusivity,

$$Km = Km_c + Bv, \quad Kh = Kh_c + Bv$$

where Km and Kh are the vertical viscosity and diffusivity used in the ocean general circulation model, respectively, Km_c and Kh_c are the original while Bv is the wave-induced vertical mixing obtained from the MASNUM wave number spectrum numerical model.

To evaluate the effects of the wave-induced mixing in the CGCMs, two numerical experiments were designed. Case 1 is FGCM-0 without wave-induced mixing, which had been run for twenty-five years, and the result of the global ocean kinetic energy demonstrated that the model achieves quasi-stationary state after ten years. Case 2 is FGCM-0 with wave-induced mixing. The wave-induced mixing was added from January 1 of the 19th model year. We will discuss the wave effects by analyzing the results of three years from the 19th to the 21st.

2 Discussion of model results

Annual mean simulated SST averaged for the equatorial 2°N—2°S strip is shown in Fig. 2, along with the climatological annual mean from Levitus data. The two cases as described above successfully approximate the east-west gradient of SST. However, the deviation of the simulation results in Case 1 is more obvious, especially in the western and central equatorial Pacific. The simulation result is 3℃ colder

in the west of the dateline than that of Levitus data. Moreover the simulated SST of the eastern Pacific (130°W—80°W) are more than 1℃ higher than the observation, especially in 120°W and 90°W, where the simulated SST is overestimated by as much as 2℃. Compared with Case 1, Case 2 shows significant improvement in its simulation of the tropical Pacific. Between 130°E and 130°W, the SST simulated by Case 2 is higher than that of Case 1, specifically between 150°E and 150°W. West of dateline, the modeled SST by Case 2 is 1.0℃ higher. Between 130°W and 80°W, the SST simulated by Case 2 is lower by 0.5℃ than Case 1, especially in the area between 120°W and 90°W where the simulated SST is lower by 0.8℃. There is a decreasing trend of SST, which is accordant with Levitus data. From 170°E to 100°W in the simulation result of Case 2, though not enough, while the trend is not observed in Case 1.

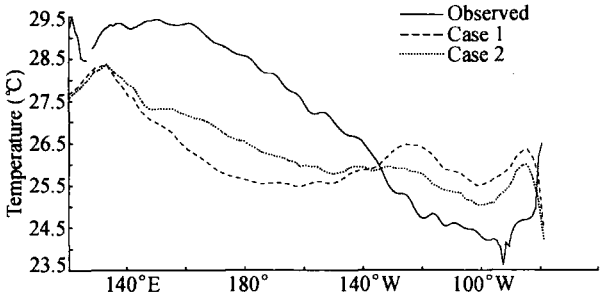

Fig. 2. Annual mean SST for the equatorial strip 2°N—2°S.

Fig. 3 shows the distribution of the SST in the tropical Pacific. As seen in Fig. 3(b), the warm pool is divided into the northern and southern warm water bands by the cold tongue extending westward from the eastern Pacific. The southeast Pacific and east of ITCZ (adjacent to the eastern coast of Pacific) is warmer than the observation. The east of 150°W and the region between 5°S and 15°S show a warm bias of about 1℃, or up to 2℃ over the area of 125—115°W, 4—6°S. There is a warm bias about 1℃ in the Peru coastal region. However, the simulated SST of Case 1 shows obvious cold bias north of 10°N and south of 15°S, and especially in the north Pacific where the cold bias area covers 90 degrees (from 140°E to 130°W). There is also a cold bias of about 2℃ located in the region between 160°E and 160°W. Simulated SST is too cold in the warm pool area where the magnitude of the bias reaches 3℃ (160—180°E, 0—3°N). Fig. 3(d) shows the simulated SST of Case 2 with *Bv*, and the results demonstrate considerable improvement over that of Case 1 without *Bv*. In the East Pacific, near Peru, the simulated SST with *Bv* is lower, e.g., up to 0.8℃ lower than those without *Bv* over the area of (5—10°N)(Fig. 3(c)). Over the area east of 150°W and south of the equator, the simulated SST is colder than those of Case 1, e.g., up to 0.8℃ over the region of 125—115°W, 0—3°S. Compared with those of Case 1, the simulated SST of Case 2 increases in the north of equator, with an improvement of more than 1℃ over the area of 170°E and 0°N. The simulated SST of Case 2 is warmer in the warm pool and the northern Pacific than that of Case 1, where the SST shows a cold bias. Over the area of 160—180°E and 0—3°N, the simulated SST increases by as much as 0.8℃—1.2℃.

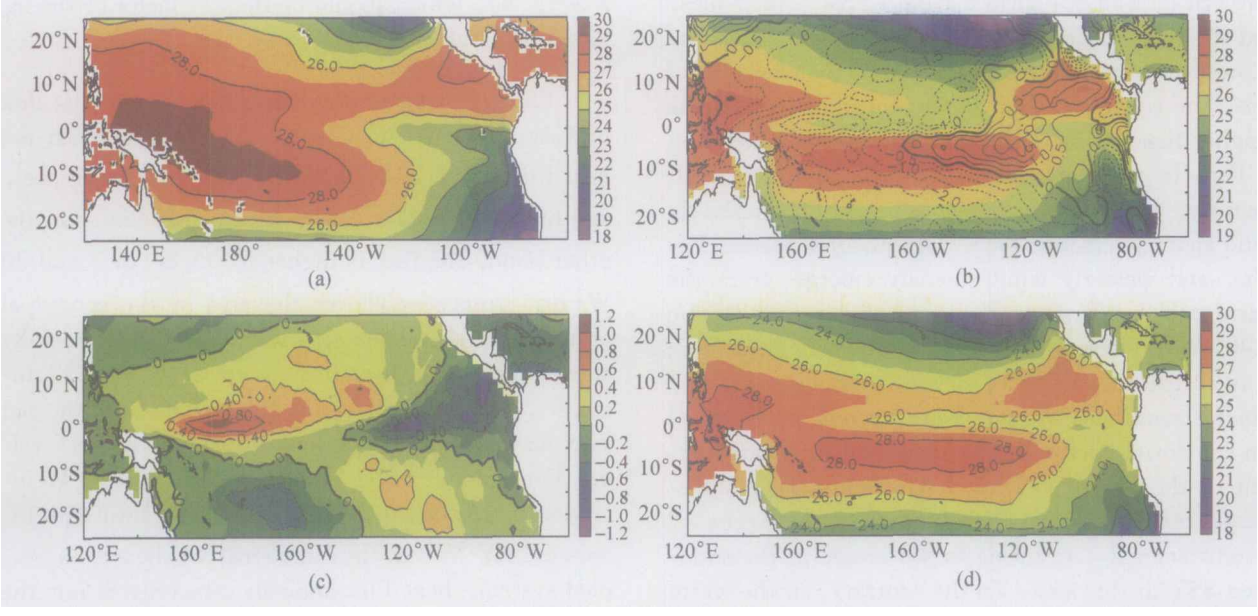

Fig. 3. The spatial distributions of annual mean SST(℃). (a) Levitus data; (b) simulation of Case 1 is represented by the shade, and counters denote SST deviation to Levitus data; (c) the difference of the SST simulations of Case 2 to Case 1; (d) simulation of Case 2.

In order to illustrate the effect of Bv clearly, we define

$\alpha_1 = |SST_{Case1} - SST_{Levitus}|$, simulated SST of Case 1 relative to Levitus data;

$\alpha_2 = |SST_{Case2} - SST_{Levitus}|$, simulated SST of Case 2 relative to Levitus data;

$\alpha = \alpha_1 - \alpha_2$, α_1 relative to α_2;

$\alpha > 0$, positive effect with Bv;

$\alpha < 0$, negative effect with Bv.

Fig. 4 shows the distribution of α in the tropic Pacific. The α is basically positive, indicating an improvement in the simulation when wave-induced mixing is taken into account. The improvement is over 0.1℃ over the region of 150°E—130°W and 5°S—25°N, and up to 0.6℃ over the area of 150°E—170°W and 5°S—5°N. The modeled SST increases by more than 0.8℃ with a maximum of 1.2℃ in the eastern Pacific (165—175°E, 0—3°N). From the above analysis, the overly westward extension of the simulated equatorial cold tongue can be successfully suppressed with the incorporation of wave-induced mixing in the coupled model, and the resulting improvement in SST simulation is much larger in the north tropical Pacific than that of the south tropical Pacific.

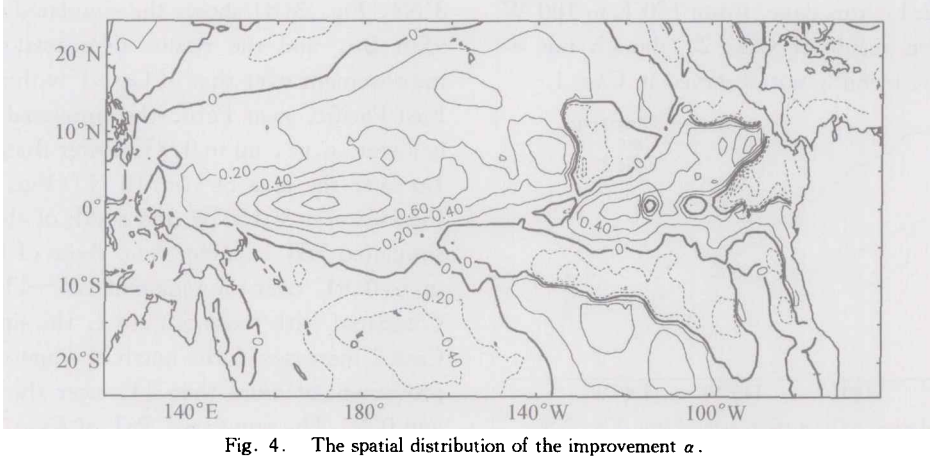

Fig. 4. The spatial distribution of the improvement α.

In order to better understand how the SST responds to the model with or without the incorporation of wave-induced mixing, the simulated sea level pressure (SLP) and sea surface wind (SSW) anomalies, and the sea surface current are shown in Figs. 5 and 6, respectively. The SLP drops in the warm pool area, the equatorial cold tongue and northern Pacific (higher than 20 Pa), while it increases off the coast of Peru in the eastern Pacific. Related to the SLP anomaly, the SSW anomaly appears. The easterly wind anomaly emerges from the equatorial eastern Pacific, and westerly wind anomaly emerges from the warm pool converge in the equatorial center Pacific (140°W). The sea surface wind anomaly field leads to the offshore sea surface current anomaly (Fig. 6), which strengthens the westward current in the eastern equatorial Pacific but weakens the westward current in the warm pool area. Upwelling anomaly emerges off the coast of Peru because of the westward current anomaly, resulting in a decrease in the simulated SST in this area. To the contrary, in the warm pool area the simulated SST increases, due at least partially to the eastward current anomaly. The convergence of the sea surface current west of the dateline yields the downwelling anomaly (160°E—160°W, 3°S—3°N), which should be the key factor of the inflated SST values.

Fig. 7 compares the distribution of net heat flux by Case 2 relative to Case 1. The annual mean net heat flux is lower by 20 $W \cdot m^{-2}$ over the warm pool, and by 30 $W \cdot m^{-2}$ over the west of dateline. On the other hand, the flux is higher by 15 $W \cdot m^{-2}$ and 30 $W \cdot m^{-2}$ respectively over the area of the equatorial eastern Pacific and the area west of 90°W. Generally speaking, the net heat flux decreases as the SST increases, or *vice versa*. But the variation of the net heat flux does not correspond utterly to the SST value. For example, SST at 15—25°S, 120—90°W increases more than 0.2℃ while the net heat flux increases 5 $W \cdot m^{-2}$ in the same area. In the air-sea coupled system, heat flux anomaly generally is not the cause but rather the result of the improvement in the

simulated SST value when the factor of wave-induced mixing is taken into consideration.

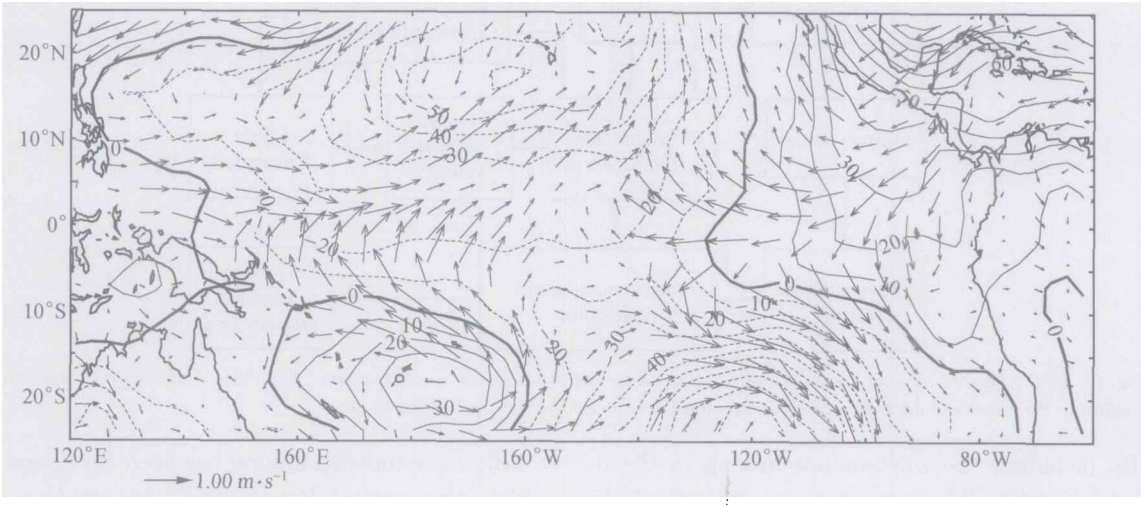

Fig. 5. The differences of sea level pressure (contoured, Pa) and sea surface wind (vector) of Case 2 to Case 1.

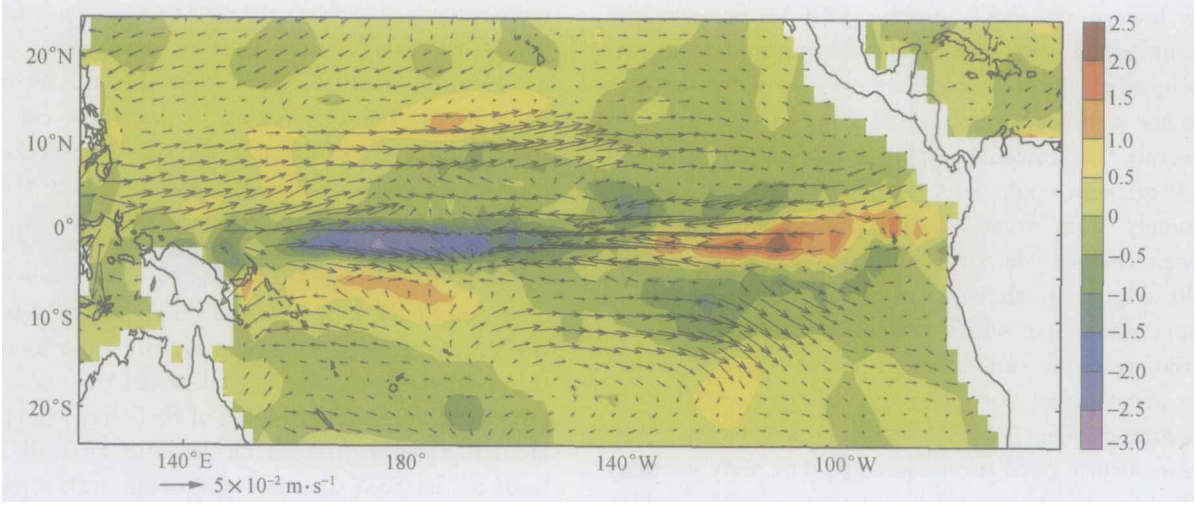

Fig. 6. The differences of the ocean surface vertical velocity (shade, 10^{-6} m·s^{-1}) and sea surface ocean current (vector) of Case 2 to Case 1.

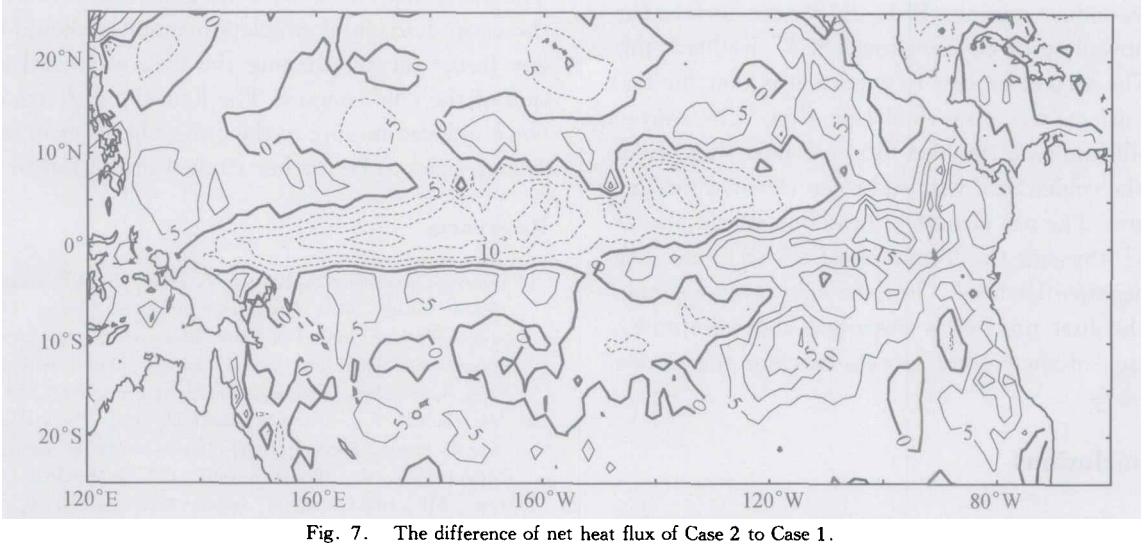

Fig. 7. The difference of net heat flux of Case 2 to Case 1.

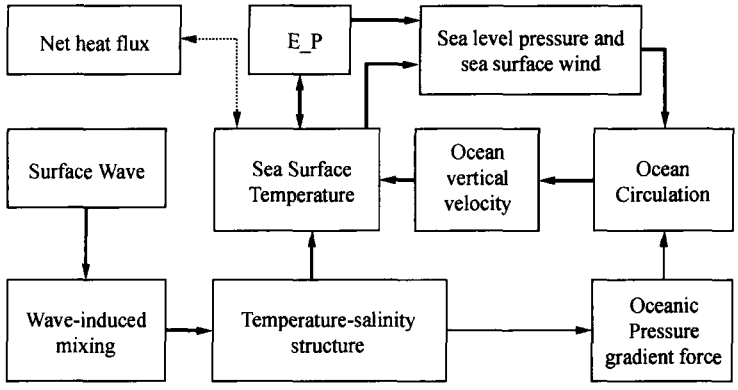

Fig. 8. The schematic view of the wave mixing effect in an atmosphere-ocean coupled system. The thick, thin and dash lines are the dominant, the minor and negative processes respectively for the cold tongue improvements.

By including the wave-induce mixing in the ocean model of CGCM, two processes will affect the SST simulation results. First, the wave-induced mixing lowers the SST in the OGCM because the strengthened vertical mixing can bring more cold water upward. In an atmosphere-ocean coupled system, the non-uniformity of the SST drop in the space can generate the horizontal gradient of SLP. The resulted SLP gradient could lead further to the surface wind anomaly and ocean surface circulation anomaly, which restrain the over-westward extension of the cold tongue into the tropical Pacific. The variation of temperature and salinity structures will lead to the variation of pressure gradient which can also induce the upper circulation anomaly. But the variation of pressure gradient should not be the key factor of the ocean surface circulation anomaly. The SSW anomaly will drive the horizontal circulation anomaly, which results in the convergence and divergence anomaly, and thus the appearance of the SST anomaly. This is a "Wave-induce mixing, SLP, SSW, sea surface current, upwelling or downwelling, SST" feedback process. The second process in operation is that the SST change affects the air-sea net heat flux. The warmer SST will lead to a lessened local net heat flux. Likewise, the colder SST will lead to an elevated local net heat flux. The net change in heat flux would also affect SST through the formation of a "SST, net heat flux" negative feedback. For the cold tongue simulation, the first process as described above improves, while that of the second process worsens the simulation results.

3 Conclusions

In this study, the coupled ocean-atmosphere general circulation model, FGCM-0, incorporated with wave-induced mixing has been developed to simulate the tropical Pacific SST. In previous studies, the simulated equatorial cold tongue without flux correction tends to be too strong, narrow, and extends overly westward. Results from an analysis of the model results of three years show that the incorporation of wave-induced mixing in the model can effectively resolve the problem of the overly extended cold tongue, and also reduce the magnitude of the cold bias in the north Pacific.

The process analysis indicates that the wave-induced mixing lowers the SST in the OGCM because the strengthened vertical mixing can bring more cold water upward. In the coupled model the non-uniformity of the space distribution of SST drops can generate a horizontal gradient of the SLP anomaly. This leads to the SSW anomaly and ocean surface circulation anomaly which can restrain the over-westward extension of the cold tongue in the tropical Pacific. The upwelling and downwelling anomalies induced by the ocean horizontal circulation anomaly should be the key factor for suppressing the over-westward extension of the cold tongue. The long-term effects of the wave-induced mixing in the atmosphere-ocean coupled system need to be further studied in the future.

References

1 Covey C, Joussaume S, Kattsov V, et al. Model Evaluation. In: Climate Change 2001, The Science of Climate Change. Contribution of Working Group 1 to Third Assessment Report of the Intergovernmental Panel on Climate Change, United Kingdom and USA. Cambridge: Cambridge University Press, 2001, 881

2 Mechoso CR, Robertson AW, Barth N, et al. The seasonal cycle over the tropical Pacific in coupled ocean-atmosphere general circulation models. Mon Wea Rev, 1995, 123: 3825—3838

3 Davey MK, Huddelstone M, Sperber KR, et al. STOIC: a study of coupled model climatology and variability in tropical ocean regions. Climate Dyn, 2002, 18: 403—420

4 Bretherton C. CLIVAR/CCSM Tropical Biases Workshop, May 28—30, 2003, GFDL. http://www.usclivar.org/Meeting_Files/PanAm_0903/EPIC_tropbias_Bretherton.pdf

5 Schneider N and Barnet TP. Indonesian throughflow in a CGCM. J Climate, 1997, 11: 676—689

6 Guilyardi E and Madec G. Performance of the OPA/ARPEGE-T21 global ocean-atmosphere coupled model. Climate Dyn, 1997, 13: 149—165

7 Boville BA, and Gent PR. The NCAR climate system model, version one. J Climate, 1998, 11(6): 1115—1130

8 Covey C, Achutarao KM, Cubasch U, et al. An overview of results from the Coupled Model Intercomparison Project. Global Planet Change, 2003, 37: 103—133

9 Sausen R, Barthels K, Hasselmann K, et al. Coupled ocean-atmosphere models with flux correction. Climate Dyn, 1988, 2: 154—163

10 Murphy JM. Transient response of the Hadley Centre coupled ocean-atmosphere model to increasing carbon dioxide. Part I: Control climate and flux adjustment. J Climate, 1995, 8: 36—56

11 Roberts CM, Gordon C and Cooper C. The origin of flux adjustments in a coupled model. Mon Wea Rev, 1997, 125: 909—925

12 David NJ and Henk A. Ocean-atmosphere interaction and the tropical climatology. Part I: The dangers of flux correction. J Climate, 1995, 8: 1325—1342

13 Meehl DA. Modification of surface fluxes from component models in global coupled models. J Climate, 1997, 10: 2811—2825

14 Philander SGH and Halpern D. Why the ITCZ is mostly north of the equator. J Climate, 1996, 9: 2958—2972

15 Ma CC, Mechoso CR, Robertson AW, et al. Peruvian stratus clouds and the tropical Pacific circulation: A coupled ocean-atmosphere GCM study. J Climate, 1996, 9: 1635—1646

16 Yu YQ, Yu RC, Zhang XH, et al. A flexible coupled ocean-atmosphere general circulation model, Adv Atmos Sci, 2002, 19(1): 169—190

17 Zhang XH, Yu YQ, Yu RC, et al. The development and application of the oceanic general circulation models. Part I: the global oceanic general circulation models. Atmos Sci (in Chinese), 2003, 27(6): 949—970

18 Alford MH. Improved global maps and 54-year history of wind work on the ocean inertial motions, Geophys Res Lett, 2003, 30 (8): 1424—1427

19 Wang W and Huang R. Wind energy input into the surface waves. J Phys Oceanogr, 2004, 34: 1276—1280

20 Wunsch C. The work done by the wind on the oceanic general circulation. J Phys Oceanogr, 1998, 28: 2331—2339

21 Qiao FL, Yuan YL, Yang YZ, et al. Wave-induced mixing in the upper ocean: Distribution and application to a global ocean circulation model. Geophys Res Lett, 2004a, 31: L11303

22 Qiao FL, Ma J, Xia CS, et al. Influence of the surface wave-induced and tidal mixing on vertical temperature structure of the Yellow and East China seas in summer. Progress in Natural Science, 2004, 16(7): 739—746

23 Jin XZ, Zhan XH, Zhou TJ, et al. Fundamental framework and experiments of the third generation of IAP/LASG world ocean general circulation model. Adv Atmos Sci, 1999, 16(2): 197—215

24 Yu YQ, Izard A, Zhang HX, et al. The response of IAP/LASG OGCM to wind stress. Atmos Sci (in Chinese), 2001, 25(6): 721—739

25 Kiehl JT, Hack JJ, Banon GB, et al. The National Center for Atmospheric Research Community Climate Model: CCM3. J Climate, 1998, 11(6): 1131—1149

26 Gent PR and McWilliams JC. Isopycnal mixing in ocean circulation models. J Phys Oceanogr, 1990, 20: 150—155

27 Pacanowski RC and Philander SGH. Parameterization of vertical mixing in numerical models of tropical oceans. J Phys Oceanogr, 1981, 11: 1443—1451

28 Yuan YL, Pan ZD, Hua F, et al. LAGDF-WAM numerical wave model. Acta Ocenologica Sinica, 1991, 10: 483—488

29 Yang YZ, Qiao FL, Zhao W, et al. MASNUM ocean wave numerical model in spherical coordinates and its application. Acta Oceanologica Sinica (in Chinese), 2005, 27(2): 1—7

30 Yu WD, Qiao FL, Yuan YL, et al. Numerical modeling of wind and waves for Typhoon Betty(8710). Acta Oceanologica Sinica, 1997, 16(4): 459—473

31 Qiao FL, Ma J, Yang YZ, et al. Simulation of the temperature and salinity along 36°N in the Yellow Sea with a wave-current coupled model. Journal of the Korean Society of Oceanography, 2004, 39(1): 35—45

32 Qiao FL, Chen SN, Li CX, et al. The study of wind, wave, current extreme parameters and climatic characters of the South China Sea. Journal of Marine Technology Society, 1999, 33(1): 61—68